Response to Referee Comments on "Interpreting Space-Based Trends in Carbon Monoxide"

Reviewer comments are in blue, and the response in black.

Response to Reviewer 1:

The manuscript describes a small series of numerical experiments to understand pre- viously reported trends in column CO from the MOPITT satellite instrument. It is a thoughtful interpretation of the MOPITT data. The manuscript would benefit from more detail in places, detailed below, but it is suitable for publication in ACP.

We thank the referee for the review and respond to individual comments below.

Detailed comments:

1) The manuscript title would benefit from being more specific.

We updated the title to: "Interpreting Space-Based Trends in Carbon Monoxide with Multiple Models"

2) MACCCity or MACCCITY? Be consistent.

We now use MACCity throughout the manuscript.

3) This reader thought the abstract would benefit from being punchier. What is the punchline? Is it that getting column ozone right is important for understanding column CO trends?

We added the following sentences to the abstract to emphasize our conclusions: "This demonstrates that biases in a model's average concentrations can influence the interpretation of the temporal trend compared to satellite observations." and "These results demonstrate that accurately simulating variability in the ozone column is important for simulating and interpreting trends in CO."

4) Line71. It would be useful for the reader to be more specific about assumptions/data used to build MACCCity. Maybe a few sentences so the reader is not required to immediately chase up details elsewhere.

We added the following details in section 2.2: "The MACCity inventory linearly interpolates the decadal anthropogenic emissions from the ACCMIP inventory (Lamarque et al., 2010) for 2000, and the RCP8.5 emissions for 2005 and 2010, to each year in between. The MACCity biomass burning emissions have year-to-year variability based on the GFED-v2 (van der Werf et al., 2006) inventory."

5) Line section 2.1. This reader believes it would be useful to show an example MO- PITT averaging kernel. Just for my own curiosity, is there a difference in the

averaging kernel over eastern China during 2010?

We added a supplemental figure showing the column averaging kernels for 2010 and two other years. We added this discussion to Section 2.1: "Supplemental Figure S1 shows the MOPITT column averaging kernels averaged over four regions. The column averaging kernels depend on the observed scene, and vary year to year as well as seasonally. The dependence of the column averaging kernels on the CO mixing ratio profile (Deeter, 2009) explains the high values in the lower troposphere over eastern China in winter." Although the kernel over eastern China varies year to year, we did not find 2010 to be fundamentally different from other years.

6) Line 90: What did the authors assume when calculating the autocorrelation?

We clarify that we calculated the autocorrelation for a 1-month lag.

7) Line 91: By deseasonalizing the column data by fitting sines/cosines the authors are implicitly assuming stationarity of these data. Do the authors believe this is a valid assumption over a decade-long time series during which the phase and amplitude of the seasonal cycle changes?

Although there are anomalies in particular months that cause year-to-year variability in the seasonal cycle, we did not find a systematic change in the phase and amplitude of the seasonal cycle.

8) Line 93: Months with insufficient data? How do the authors define this criterion?

We now clarify: "Months with no MOPITT data or only a few days of MOPITT data are excluded from the trend analysis. This includes May-August of 2001 and August-September of 2009."

9) Line 95: Do the authors sample the model along the orbit tracks?

We use the level 3 data, which is a gridded product. We added this information in section 2.1.

10) Minor comment: a few instances where the references should be inline but are not. I expect the typesetting process will pick this up.

Fixed.

11) Section 2.2: Would be useful if the authors provide some regional emission estimates of CO, particularly for pertinent regions.

We added the following information: "From 2000 to 2010, CO emissions in the MACCity inventory decreased from 31 to 11 Tg yr^{-1} over the eastern U.S., from 97 to 59 Tg yr^{-1} over Europe, and increased from 56 Tg to 72 Tg yr^{-1} over eastern China."

12) Equation 1. The usual convention is lower-case bold typeface for vectors and upper-case bold typeface for matrices.

We modified the equation to reflect this convention.

13) This reader is confused why the authors included two sets of statistics: 2000-2010 and 2000-2011. If the results from these two sets had been significantly different I would have probably suggested a major re-analysis of the data. But they are not so I suggest (and only suggest) the authors summarize the value of the additional data in a few sentences and report only 2000-2010.

We updated the text and figures to report only values for 2000-2010, and removed the supplemental figure, which showed results for 2000-2011. We added the following sentence to Section 2.2: "Some simulations were available through 2011, while others ended in 2010. We therefore report results for 2000-2010, but note that extending the analysis through 2011 does not alter the conclusions."

14) Line 186 and elsewhere: The authors won't need reminding that a model-data correlation r of just over 0.7 is required for the model to describe 50% of the observed variation. In some places the authors extol correlations of X (much less than 0.7) while in other places the author extol the squared correlation values of Y.

We agree that many of the r values shown in Table 2b are below 0.7 and thus imply that the simulations are capturing less than half of the variance. However, we find it useful to report and discuss these r values to indicate the relative performance of different simulations. We updated this table to indicate which correlations are statistically significant. We updated the text in Section 3.3 to report r values rather than r^2 for consistency with the rest of the paper.

15) Line 265: What is responsible for the observed and model total column anomaly in 2010?

Steinbrecht et al. (2011) attribute the 2010 anomaly in northern midlatitude ozone observations to a combination of an unusually strong negative Arctic Oscillation and North Atlantic Oscillation and the easterly phase of the quasi-biennial oscillation. We added this information in Section 3.3.

16) Line 271: "can be" or "is"?

We changed this to "is partially".

Response to Referee 2:

The authors have used a series of chemistry-climate and chemical transport model simulations to understand the negative trends in CO observed by MOPITT. They find that the negative trend in the bottom-up inventories reproduce the trend observed

over North America and Europe, but is incapable of capturing the negative trend observed over China. They attributed the discrepancies between the modeled and observed trend in CO over China to changes in the MOPITT vertical sensitivity and to biases in the modeled ozone abundances, which produces a bias in modeled OH and, thus, CO. The paper is well written and the authors did a careful analysis of the trends in the models. I would recommend publication in ACP after the authors have revised the manuscript to address my comments below.

We appreciate the thoughtful review and respond to comments below.

Comments

1) Line 85: The Level 3 MOPITT data are daily or monthly gridded data. Are the authors using the daily gridded data here? Are they using nighttime and daytime, or just daytime data? If they are using Level 3 data, how do they compare the model to the MOPITT data. The model should be sampled at the MOPITT observation locations and times when transforming the model with the MOPITT averaging kernels and a priori profiles. They need to better explain in the paper how this is done.

We now clarify in section 2.1 that we are using the monthly gridded daytime data, and that the level 3 product includes the averaging kernel and a priori for each grid box. In section 2.2, we added that we regrid the model results to the MOPITT grid. We expect the error from using monthly mean simulated CO instead of sampling at the overpass time to be small since CO does not have a large diurnal cycle. Our analysis includes a free-running CCM simulation as well as CTM simulations. The meteorology of the free-running CCM will not match up with the observed for individual days, and our focus is on monthly and interannual rather than daily variability, so we chose to use the monthly mean MOPITT product. Martinez-Alonso et al [2014] demonstrated that there is only a small bias from using gridded average averaging kernels rather than the kernels of individual retrievals.

2) Lines 137 – 141: In giving Equation (1), the authors should explain that the MOPITT retrievals are with respect to the log of the mixing ratio and they should also cite Deeter (2009) "MOPITT (Measurements of Pollution in the Troposphere) Validated Version 4 Product User's Guide" for providing guidance for calculating the column averaging kernels from the averaging kernels that is with respect to the log of the mixing ratio.

We added the following line to Section 2.2: "The column averaging kernel is calculated from the standard averaging kernel matrix, which is based on the log of the CO concentration profile, following the method of Deeter (2009):

$$a_j = (K / \log_{10}e) \sum \Delta p_i \, v_{rtv,i} \, A_{ij} \qquad (2)$$

where Δp_i and $v_{rtv,i}$ are the pressure thickness and retrieved CO concentration, respectively, of level i, $\mathbf{A}$ is the standard averaging kernel matrix, and $K = 2.12 * 10^{13}$

molec cm^{-2} hPa^{-1} ppb^{-1}."

3) Lines 201-203: The authors state here that the discrepancy is "driven largely by the failure of the simulations to capture the 2008 dip," but the models are also strongly biased in 2010, for example (Fig. 2f). Indeed, this 2010 bias is the focus of the ozone analysis in Figs. 3 and 4.

We added: "leading to an overestimate that continues through 2010".

4) Please state the regional boundaries for the regions considered in Fig. 2.

We added this information to the caption of Fig. 2.

5) Lines 226 – 244: I find this discussion confusing. I understand how time-dependent variations in the vertical sensitivity of the MOPITT retrievals could contribute to trends in the data. But I don't understand how, as stated on Lines 228-321, the bias in the modeled CO can produce an artificial trend. It seems to me that there are two possible way this could happen:

a) Are the authors suggesting that changes in the vertical distribution of the model bias, combined with the varying vertical sensitivity of the MOPITT retrievals, produces an artificial trend when the model is convolved with the averaging kernels and a priori profile?

b) If the model bias is constant in time, then the convolved modeled columns should exhibit the same trend as the data. The presence of a fixed bias in the model together with temporally varying averaging kernels should only impact the trend if the biased model state is so far from the a priori MOPITT state that the linearization assumption in Equation (1) is invalid i.e., the averaging kernels do not accurately capture the sen- sitivity of the retrieval between the modeled state and the MOPITT a priori. Is this what the authors are trying to say on lines 226-228?

The authors need to explain more clearly how the bias in the model could be contribut- ing to an artificial trend.

As the reviewer suggests in a), the bias in CO varies with altitude, so if the vertical sensitivity described by the averaging kernel changes to e.g. place more weight on higher altitudes, this will change the value of the convolved CO column even if there were no changes in the CO profile. But even if the bias were constant with altitude, changes in the averaging kernel result in more or less weight placed on the a priori versus the CO simulated by the model. Thus, a difference between the a priori and the model means that placing more (or less) weight on the a priori will change the resulting value of C_{sim}. Since the a priori profiles and columns are constant in time, taking the time derivative of equation 1 yields:

$$\partial C_{sim}/\partial t = \mathbf{a}\,(\partial \mathbf{x}_{mod}/\partial t) + \partial \mathbf{a}/\partial t\,(\mathbf{x}_{mod} - \mathbf{x}_0)$$

The second term on the right hand side shows that the larger the bias between the modeled CO and the a priori, the larger the impact of the changing averaging kernel. We now discuss this in Section 3.2.

6) Lines 261-262: Yes, we expect that anomalies in OH to be inversely related to anomalies in total ozone, however, the OH and ozone anomalies do not seen to be strongly correlated in Fig. 3. It would be helpful if the authors gave the correlation coefficient between the two quantities for different latitude bands in the tropics and extratropical northern hemisphere.

We added the following sentence to this discussion: "The correlation coefficient between OH and column ozone is -0.53 for the 15°S-15°N average, -0.72 for the 15°-25°N average, and -0.75 for the 30°-60°N average."

7) Lines 263-264: The ozone column anomaly in Fig. 3 is in the extratropical northern hemisphere, mainly in early (Jan-Mar) 2010. Although the global, annual mean CO lifetime is 1-2 months, in the extratropics in winter it could be longer than a season. If that is the case, it is unclear to me how the changes in OH in early 2010 could drive such large changes in CO between 30-60N in winter.

The early 2010 OH anomaly occurs in the northern tropics as well as the extratropics. We added the following sentence to highlight this: "This OH anomaly extends from the northern tropics to the midlatitudes." Northern midlatitude (30-60N) CO and OH are anticorrelated with an r value of -0.69. This r value increases to -.78 if we apply a three-month smoothing, reflecting the longer lifetime of CO. However, since the lifetime of CO is several months, we do not expect a one-to-one correspondence between CO anomalies and OH anomalies, and we added a sentence stating this. We also clarified figure 3 by adding the units to each panel.

8) Figure 4: The 2010 ozone anomaly is about 5%. What are the altitude ranges that are contributing to this bias in the column? Are these changes mainly in the UTLS?

The 2010 anomaly in both the SBUV data and the model is driven by ozone at pressures higher than 25hPa. The vertical resolution of the SBUV data does not allow us to determine the specific altitude of the bias. However, comparison to MLS data shows that GMI has a high bias in lower stratospheric ozone (pressures greater than 50 hPa) in the first half of 2010.

Technical comments

1. Line 64: Change "results of (Li and Liu, 2010)" to "results of Li and Liu (2010"

Fixed

2. Figure 2: It difficult to see the seven different lines in each panel. If the authors remove the titles on the y-axes on the panels in the right column and reduce the spacing between the panels, it may be possible to enlarge each panel to make the

plots more legible.

We updated this figure as suggested.

Interpreting Space-Based Trends in Carbon Monoxide with Multiple Models

Sarah A. Strode[1,2], Helen M. Worden[3], Megan Damon[2,4], Anne R. Douglass[2], Bryan N. Duncan[2], Louisa K. Emmons[3], Jean-Francois Lamarque[3], Michael Manyin[2,4], Luke D. Oman[2], Jose M. Rodriguez[2], Susan E. Strahan[1,2], Simone Tilmes[3]

[1]Universities Space Research Association, Columbia, MD, USA
[2]NASA Goddard Space Flight Center, Greenbelt, MD, USA
[3]National Center for Atmospheric Research, Boulder, CO, USA
[4]Science Systems and Applications, Inc., Lanham, MD, USA

Correspondence to: S. A. Strode (sarah.a.strode@nasa.gov)

Abstract

We use a series of chemical transport model and chemistry climate model simulations to investigate the observed negative trends in MOPITT CO over several regions of the world, and to examine the consistency of time-dependent emission inventories with observations. We find that simulations driven by the MACCity inventory, used for the Chemistry Climate Modeling Initiative (CCMI), reproduce the negative trends in the CO column observed by MOPITT for 2000-2010 over the eastern United States and Europe. However, the simulations have positive trends over eastern China, in contrast to the negative trends observed by MOPITT. The model bias in CO, after applying MOPITT averaging kernels, contributes to the model-observation discrepancy in the trend over eastern China. This demonstrates that biases in a model's average concentrations can influence the interpretation of the temporal trend compared to satellite observations. The total ozone column plays a role in determining the simulated tropospheric CO trends. A large positive anomaly in the simulated total ozone column in 2010 leads to a negative anomaly in OH and hence a positive anomaly in CO, contributing to the positive trend in simulated CO. These results demonstrate that accurately simulating variability in the ozone column is important for simulating and interpreting trends in CO.

1. Introduction

Carbon monoxide (CO) is an air pollutant that contributes to ozone formation and affects the oxidizing capacity of the troposphere (Thompson, 1992; Crutzen, 1973). Its primary loss is through reaction with OH, which leads to a lifetime of 1-2 months (Bey et al., 2001) and makes CO an excellent tracer of long-range transport. Both fossil fuel combustion and biomass burning are major sources of CO. The biomass burning source shows large interannual variability (van der Werf et al., 2010), while fossil fuel emissions typically change more gradually. The time-dependent MACCity inventory (Granier et al., 2011) shows decreases in CO emissions from the United States and Europe from 2000 to 2010 due to increasing pollution controls, but increases in emissions from China. MACCity emissions for years after 2000 are based on the Representative Concentration Pathway (RCP) 8.5 (Riahi et al., 2007). The REAS (Kurokawa et al., 2013) and EDGAR4.2 (EC-JRC/PBL, 2011) inventories also show increasing CO emissions from China. The bottom-up inventory of Zhang et al. (2009) shows an 18% increase in CO emissions from China from 2001 to 2006, and Zhao et al. (2012) estimate a 6% increase between 2005 and 2009. However, there is considerable uncertainty in bottom-up inventories, and comparison of model hindcast simulations driven by bottom-up inventories with observations provides an important test of the time-dependent emission estimates.

Space-based observations of CO are now available for over a decade and show trends at both hemispheric and regional scales. Warner et al. (2013) found significant negative trends in both background CO and recently emitted CO at 500 hPa over southern hemisphere oceans and northern hemisphere land and ocean in Atmospheric Infrared Sounder (AIRS) data. Worden et al. (2013) calculated trends in the CO column from several thermal infrared (TIR) instruments including MOPITT and AIRS. They found statistically significant negative trends over Europe, the eastern United States, and China for 2002-2012. He et al. (2013) also report a negative trend in MOPITT near-surface CO over western Maryland.

Surface concentrations of CO show downward trends over the United States driven by emission reductions (EPA, 2011), consistent with the space-based trends. Decreases in the partial column of CO from FTIR stations in Europe also show decreases from 1996 to 2006, consistent with emissions decreases (Angelbratt et al., 2011). Yoon

Deleted:

and Pozzer (2014) found that a model simulation of 2001 to 2010 reproduced negative trends in surface CO over the eastern U.S. and western Europe, but showed a positive trend in surface CO over southern Asia.

The cause of the negative trend over China seen in MOPITT and AIRS data is uncertain. The trend is consistent with the results of Li and Liu (2011), who found decreases in surface CO measurements in Beijing, and with decreases in CO emissions in 2008 inferred from the correlation of CO with CO_2 measured at Hateruma Island (Tohjima et al., 2014) and at a rural site in China (Wang et al., 2010). Yumimoto et al. (2014) used inverse modeling of MOPITT data to infer a decrease in CO emissions from China after 2007. The 2008 Olympic Games and the 2009 global economic slowdown led to reductions in CO (Li and Liu, 2011; Worden et al., 2012). However, the negative trend in MOPITT CO is inconsistent with the rising CO emissions of the MACCity and REAS inventories. Inverse modeling of MOPITT version 6 data yields a negative trend in CO emissions from China and a larger global decline in CO emissions than that found in the MACCity inventory (Yin et al., 2015).

This study examines whether global hindcast simulations can reproduce the trends and variability in carbon monoxide seen in the MOPITT record. We examine the role of averaging kernels and the contribution of trends at different altitudes to the trends observed by MOPITT. We then examine the impact of OH variability on the simulated trends in CO.

Deleted: (

Deleted: ,

2. Methods

2.1. MOPITT

The MOPITT instrument onboard the Terra Satellite provides the longest satellite-based record of atmospheric CO, with observations available from March 2000 to present. It provides nearly global coverage every three days (Edwards et al., 2004). We use the monthly Level 3 daytime column data from the Version 5 TIR product, which has negligible drift in the bias over time (Deeter et al., 2013). The level 3 data is a gridded product and includes the a priori and averaging kernel for each grid box. Supplemental Figure S1 shows the MOPITT column averaging kernels averaged over four regions. The column averaging kernels depend on the observed scene, and vary year to year as well as

seasonally. The dependence of the column averaging kernels on the CO mixing ratio profile (Deeter, 2009) explains the high values in the lower troposphere over eastern China in winter.

We calculate trends and de-seasonalized anomalies for the Eastern U.S., Europe, and eastern China regions described by Worden et al. (2013). Trends that differ from zero by more than the two-sigma uncertainty on the trend are considered statistically significant. We account for autocorrelation of the data for a one-month lag when calculating the uncertainty on the trends. We calculate the annual cycle by fitting the data with a series of sines and cosines as well as the linear trend, and then remove the annual cycle to obtain the de-seasonalized anomalies. Months with no MOPITT data or only a few days of MOPITT data are excluded from the trend analysis. This includes May-August of 2001 and August-September of 2009. We report the MOPITT trends for 2000-2010 for comparison with model simulations, and for 2000-2014 to give a longer-term view of the observed trends.

Deleted: with insufficient data

Deleted: and 2000-2011

2.2. Model Simulations

We use a suite of chemistry climate model (CCM) and chemical transport model (CTM) simulations to interpret the observed trends. The Global Modeling Initiative (GMI) CTM includes both tropospheric (Duncan et al., 2007) and stratospheric (Strahan et al., 2007) chemistry, including over 400 reactions and 124 chemical species. Meteorology for the GMI simulations comes from the Modern-Era Retrospective Analysis for Research and Applications (MERRA) (Rienecker et al., 2011). The GEOS-5 Chemistry Climate Model (GEOSCCM)(Oman et al., 2011) incorporates the GMI chemical mechanism into the GEOS-5 atmospheric general circulation model (AGCM). The GEOSCCM simulations are forced by observed sea surface temperatures (SSTs) from (Reynolds et al., 2002).

The Community Earth System Model, CESM1 CAM4-chem, includes 191 chemical tracers and over 400 reactions for both troposphere and stratosphere (Tilmes et al., 2016). The model can be run fully coupled to a free-running ocean, with prescribed SSTs, or with nudged meteorology from GEOS-5 or MERRA analysis. CESM1 CAM4-chem is

129 further coupled to the land model, providing biogenic emissions from the Model of
130 Emissions and Aerosols from Nature (MEGAN), version 2.1 (Guenther et al., 2012).
131 Several simulations were conducted as part of the Chemistry-Climate Model Initiative
132 (CCMI) project (Eyring et al., 2013). These include the Ref-C1 simulation of the
133 GEOSCCM and a Ref-C1 CESM1 CAM4-Chem simulation, hereafter called G-Ref-C1
134 and C-Ref-C1, respectively, and the Ref-C1-SD simulation of the GMI CTM. Both the
135 Ref-C1 and the Ref-C1-SD simulations use time-dependent anthropogenic and biomass
136 burning emissions from the MACCity inventory (Granier et al., 2011), but the Ref-C1-
137 SD simulations use specified meteorology while the Ref-C1 simulations run with
138 prescribed SSTs. The MACCity inventory linearly interpolates the decadal
139 anthropogenic emissions from the ACCMIP inventory (Lamarque et al., 2010) for 2000,
140 and the RCP8.5 emissions for 2005 and 2010, to each year in between. The MACCity
141 biomass burning emissions have year-to-year variability based on the GFED-v2 (van der
142 Werf et al., 2006) inventory. From 2000 to 2010, CO emissions in the MACCity
143 inventory decreased from 31 to 11 Tg yr^{-1} over the eastern U.S., from 97 to 59 Tg yr^{-1}
144 over Europe, and increased from 56 Tg to 72 Tg yr^{-1} over eastern China.
145 Given the uncertainty in CO emissions, we conduct a GMI CTM simulation using an
146 alternative time-dependent emissions scenario, called AltEmis. This simulation is
147 described in detail in (Strode et al., 2015b). Briefly, anthropogenic emissions include
148 time-dependence based on EPA (http://www.epa.gov/ttn/chief/trends/index.html), the
149 REAS inventory (Ohara et al., 2007), and EMEP
150 (http://www.ceip.at/ms/ceip_home1/ceip_home/webdab_emepdatabase/reported_emissio
151 ndata/), and annual scalings from van Donkelaar et al. (2008). Biomass burning
152 emissions are based on the GFED3 inventory (van der Werf et al., 2010). While the
153 regional emission trends in this simulation are of the same sign as in the Ref-C1 case, the
154 magnitude of the negative trends over the U.S. and Europe are smaller and the positive
155 trend over China is larger, leading to a positive global trend (Fig. 1). We also conduct a
156 sensitivity study called EmFix with anthropogenic and biomass burning emissions held
157 constant at year 2000 levels. Table 1 summarizes the simulations used in this study.
158 We regrid the model output to the MOPITT grid and convolve the simulated CO with
159 the MOPITT averaging kernels and a priori in order to compare the simulated and

Formatted: Superscript
Formatted: Superscript
Formatted: Superscript
Deleted: '
Deleted: (
Deleted: ,

observed CO columns. The averaging kernels are space and time dependent. We use the following equation from Deeter et al. (2013):

$$C_{sim} = C_0 + a(x_{mod} - x_0) \quad (1)$$

where C_{sim} and C_0 are the simulated and a priori CO total columns, respectively, a is the total column averaging kernel, and x_{mod} and x_0 are the modeled and a priori CO profiles, respectively. The column averaging kernel is calculated from the standard averaging kernel matrix, which is based on the log of the CO concentration profile, following the method of Deeter (2009):

$$a_i = (K / \log_{10}e) \sum \Delta p_i \, v_{rtv,i} \, A_{ij} \quad (2)$$

where Δp_i and $v_{rtv,i}$ are the pressure thickness and retrieved CO concentration, respectively, of level i, $\mathbf{A}$ is the standard averaging kernel matrix, and $K = 2.12 * 10^{13}$ molec cm^{-2} hPa^{-1} ppb^{-1}.

We deseasonalize the simulated CO columns and calculate their linear trend following the same procedure that we applied to the MOPITT CO. Months that do not have MOPITT data (June-July 2001 and August-September 2009) are excluded from the analysis of the model trends as well.

The Ref-C1 and Ref-C1-SD simulations requested by CCMI extend until 2010. However, the MACCity biomass burning emissions extend only until 2008. CAM4-Chem therefore repeated the biomass burning emissions for 2008 for years 2009-2010. In contrast, the GEOSCCM Ref-C1 and GMI Ref-C1-SD simulations used emissions from GFED3 (van der Werf et al., 2010) for years after 2008. Some simulations were available through 2011, while others ended in 2010. We therefore report results for 2000-2010, but note that extending the analysis through 2011 does not alter the conclusions.

3. Results

3.1. Trends over Europe, the United States, and the Northern Hemisphere

The hindcast simulations driven by MACCity emissions (G-Ref-C1, Ref-C1-SD, and C-Ref-C1) show negative trends in CO over the U.S. and Europe that agree with the observed slope from MOPITT within the uncertainty (Fig. 2, Table 2). The MOPITT

Deleted: (
Deleted: ,
Deleted: A
Formatted: Font:Bold
Deleted: X
Formatted: Font:Bold
Deleted: X
Formatted: Font:Bold
Deleted: W
Formatted: Font:Bold
Deleted: A
Formatted: Font:Bold
Deleted: X
Formatted: Font:Bold
Deleted: X
Formatted: Font:Not Bold, Subscript
Formatted: Subscript
Formatted: Subscript
Formatted: Subscript
Formatted: Subscript
Formatted: Indent: Left: 0"
Formatted: Subscript
Formatted: Subscript
Formatted: Font:Bold
Formatted: Superscript
Formatted: Superscript
Formatted: Superscript
Formatted: Superscript

Deleted: We also report the simulated and MOPITT trends for both 2000-2010 and 2000-2011 since some simulations are only available to 2010, while others continued through 2011. Figure S1 in the supplemental information shows results extended through 2011.

207 trends for both regions are statistically significant for both regions, as shown by Worden
208 et al. (2013). These results are consistent with the findings of Yin et al. (2015), whose
209 inversion of MOPITT data showed a posteriori trends in CO emissions over the U.S. and
210 western Europe that were consistent with but slightly larger than the a priori trends. The
211 EmFix hindcast shows a positive, though non-significant, trend for both regions,
212 indicating that the decrease in CO emissions is necessary for reproducing the downward
213 trend in the CO column. The AltEmis simulation fails to produce the negative trends,
214 despite including negative trends in regional emissions for both the U.S. and Europe.
215 The impact of these negative regional trends is insufficient to overcome the positive
216 global emission trend in the AltEmis scenario (Fig. 1), leading to positive trends in CO.
217 Figure 2 also reveals a negative bias in the simulated CO column between the models
218 and MOPITT. A low bias in simulated CO at northern latitudes is often present in global
219 models (Naik et al., 2013), and may indicate a high bias in northern hemisphere OH
220 (Strode et al., 2015a) or CO dry deposition (Stein et al., 2014), as well as an
221 underestimate of CO emissions.
222 The deseasonalized anomalies in the MOPITT and simulated CO columns are shown
223 in Fig. 2b,d, and the correlation coefficient between the observed and simulated monthly
224 anomalies are presented in Table 2b. The highest correlations are for the AltEmis and
225 Ref-C1-SD simulations of the GMI CTM. This result is consistent with the use of year-
226 specific meteorology, which we expect to better match the transport of particular years.
227 The lowest correlations are for the EmFix simulation. This is expected since the EmFix
228 simulation does not include inter-annual variability (IAV) in biomass burning. The IAV
229 in biomass burning makes a large contribution to the IAV of CO (Voulgarakis et al.,
230 2015).
231 The role of biomass burning in driving the CO variability is even more evident at the
232 hemispheric scale. Figure 2g,h shows the anomalies in MOPITT and the simulations for
233 the northern hemisphere (0-60N). The EmFix simulation shows almost no correlation,
234 while the other simulations have correlation coefficients exceeding 0.6 (Table 2). The
235 role of changing anthropogenic emissions is also evident, as the Ref-C1-SD simulation
236 captures the 2008-2009 dip in the CO column while the EmFix simulation does not.
237 Gratz et al. (2015) found decreasing CO concentrations at Mount Bachelor Observatory

in Oregon during spring for 2004-2013, which they attribute to reductions in emissions leading to a lower hemispheric background. We also note that Ref-C1-SD and G-Ref-C1 have similar correlations with the observed variability for the northern hemisphere (Table 2), indicating that transport differences are less important for variability at the hemispheric scale.

3.2. Trend over China

Observations from MOPITT show a negative trend in the CO column over eastern China for 2002-2012 (Worden et al., 2013). The negative trend for the years 2000-2014 exceeds that for 2000-2010 (Table 2), showing that it is not driven solely by temporary emission reductions in 2008. Our simulations do not reproduce this trend, and instead show increases in the CO column (Fig. 2e), which is expected given that CO emissions from China increase in four of the five simulations. The anomalies (Fig. 2f) show that the discrepancy in the simulated versus observed trends is driven largely by the failure of the simulations to capture the 2008 dip in the CO column, leading to an overestimate that continues through 2010. This suggests emission reductions in China during this time period are not adequately captured by the emission inventories. However, the good agreement between the observed and simulated decreases in CO for the northern hemisphere as a whole (Fig. 2g,h) suggest that on a global scale, the emission time series is reasonable. Consequently, we examine several other factors that may contribute to the difference in sign between the MOPITT and simulated CO trends.

Regional trends in CO are expected to vary with altitude, with surface concentrations most heavily influenced by local emissions. MOPITT TIR retrievals have higher sensitivity to CO in the mid-troposphere than at the surface (Deeter et al., 2004), so the trend in the MOPITT CO column will be weighted towards the trends in free tropospheric CO rather than near-surface CO. We quantify this impact on our Ref-C1-SD CO column trends by comparing the trend in the pure-model CO column with that of the simulated column convolved with the MOPITT averaging kernels.

The simulated CO trend over eastern China for 2000-2010 is positive (but not significant) both with and without the averaging kernels, but application of the MOPITT kernels increases the positive trend from 1.3*10^{16} molec cm^{-2} yr^{-1} to 1.4*10^{16} molec cm^{-2} yr^{-1}. This result is initially surprising since we expect trends in the mid-troposphere to be

Deleted: 1

Deleted: , S1e

Deleted: , S1f

Deleted: 1

Deleted: 0

Deleted: 3

more strongly influenced by the decrease in the hemispheric CO background. Indeed, the trends in CO concentration over eastern China simulated in Ref-C1-SD switch from positive in the lower troposphere to negative in the middle and upper troposphere. However, the application of the kernels results in more positive (or less negative) trends in all regions.

Yoon et al. (2013) show that since the averaging kernels vary over time, a bias between the true atmosphere and the a priori assumed by MOPITT can lead to an artificial trend in the retrieved CO. Similarly, the bias between the average simulated CO concentrations and the MOPITT a priori, evident in Figure 2, can lead to an artifact in the simulated CO trend when the simulation is convolved with the MOPITT averaging kernels. This is due to the changing contribution of the a priori when the vertical sensitivity (averaging kernel) is varying in time. MOPITT vertical sensitivity varies with time due to instrument degradation as well as the change in CO abundance. The bias in CO varies with altitude, so if the vertical sensitivity described by the averaging kernel changes, this will change the value of the convolved CO column even if there were no changes in the CO profile. Furthermore, changes in the averaging kernel result in more or less weight placed on the a priori versus the CO simulated by the model. Thus, a difference between the a priori and the model means that placing more (or less) weight on the a priori will change the resulting value of C_{sim}. Since the a priori profiles and columns are constant in time, taking the time derivative of equation 1 yields:

$$\partial C_{sim}/\partial t = \mathbf{a}\,(\partial \mathbf{x}_{mod}/\partial t) + \partial \mathbf{a}/\partial t\,(\mathbf{x}_{mod} - \mathbf{x}_0) \qquad (3)$$

The second term on the right hand side shows that the larger the bias between the modeled CO and the a priori, the larger the impact of the changing averaging kernel.

We quantify this effect by convolving the simulated CO for each year with the MOPITT averaging kernels for the year 2008, thus removing the effect of the time-dependence of the averaging kernels. The resulting trend, $0.56*10^{16}$ molec cm^{-2} yr^{-1}, is less positive than the pure model trend or the original simulated trend. Thus, accounting for the time-dependence of the averaging kernels convolved with model bias reduces but does not eliminate the discrepancy with the observed trend. Other regions also show a more negative trend when the same averaging kernel is applied to the model results for all years. The large bias in CO at middle and high northern latitudes commonly seen in

Deleted: and a priori via equation 1

Formatted: Indent: First line: 0"

Deleted: 42

modeling studies thus impacts the ability of models to reproduce and attribute observed trends in satellite data.

Figure 2 and Table 2 also show a positive trend in the GMI EmFix simulation for eastern China. This larger trend in the EmFix simulation than the Ref-C1-SD simulation indicates that the net decrease in emissions contributes to decreasing CO over eastern China, consistent with the observed negative trend, but other factors in the model cause an increase in CO over eastern China even when all emissions are constant. The trend in the EmFix simulation thus contributes to the erroneous sign of the trend in the GMI simulations. The trends in the EmFix simulation for the northern hemisphere average and the eastern U.S. and Europe are positive as well (Table 2). We examine their cause in the next section.

3.3. Contribution of OH Interannual Variability

Since the EmFix simulation shows a positive trend in the northern hemisphere, we next examine the variability in the CO sink, OH. We also examine variability in the total ozone column, since overhead ozone is a major driver of OH variability (Duncan and Logan, 2008). Figure 3 shows the variability in CO and OH in the EmFix simulation. The positive and negative anomalies in CO correspond with the negative and positive anomalies, respectively, in OH. The anomalies in OH are in turn inversely related to anomalies in the total ozone column. The correlation coefficient between OH and column ozone is -0.53 for the 15°S-15°N average, -0.72 for the 15°-25°N average, and -0.75 for the 30°-60°N average. The large NH ozone anomaly in 2010, in particular, leads to a large anomaly in OH and thus CO. This OH anomaly extends from the northern tropics to the midlatitudes. The large CO anomaly near the end of the time series contributes to the apparent 11-year trend. We note that since the lifetime of CO is several months, CO anomalies are not expected to have a one-to-one correspondence with the OH anomalies.

The large anomaly in the simulated total ozone column in 2010 is overestimated compared to observations. Figure 4 shows the time-dependence of the total ozone column from 30°-60°N in EmFix compared to SBUV data (Frith et al., 2014). While the observations show an anomaly in 2010, the magnitude is smaller than that produced by

the simulation. Steinbrecht et al. (2011) attribute the 2010 anomaly in northern midlatitude ozone observations to a combination of an unusually strong negative Arctic Oscillation and North Atlantic Oscillation and the easterly phase of the quasi-biennial oscillation.

While the impact of OH interannual variability on the apparent trend in CO is clear in the EmFix simulation, this source of variability is partially masked by large interannual variability in CO emissions in the other simulations. We examine the correlation between the de-trended and deseasonalized CO anomalies from 10°S-10°N in the Ref-C1-SD simulation and the CO emissions as well as the simulated OH and column ozone. Since the CO emitted in a given month can influence concentrations for several subsequent months, we use a 3-month smoothing of the emission time series. We find a high correlation ($r=0.88$) between the CO anomalies and the CO emissions. This correlation is also evident in the MOPITT data, as the MOPITT CO anomalies have a correlation of $r=0.70$ with the emissions. Figure 5 shows the strong relationship between the simulated CO anomalies and the CO emissions. However, the colors in Fig. 5 indicate that the scatter for a given level of emissions is often linked to the OH anomalies, with low/high OH anomalies leading to CO that is higher/lower than would be predicted just from the CO emissions. We find that the 10°S-10°N OH in the Ref-C1-SD simulation is anticorrelated with CO ($r=-0.62$) and with the total ozone column ($r=-0.68$). Consequently, the simulated ozone column plays a role in modulating tropical CO variability even when variable CO emissions are included, although the emissions still play the strongest role.

Deleted: can be

Deleted: 2

Deleted: 7

Deleted: 2

Deleted: 49

Deleted: 2

Deleted: 33

Deleted: 2

Deleted: 45

4. Conclusions

We conducted a series of multi-year simulations to analyze the causes of the negative trends in MOPITT CO reported by Worden et al. (2013). Both CTM and CCM simulations driven by the MACCity emissions reproduce the observed trends over the eastern U.S. and Europe, providing confidence in the regional emission trends.

Deleted: (

Deleted: ,

None of the simulations reproduce the observed negative trend over eastern China. This negative trend persists even with the MOPITT data extended out to 2014. The MOPITT averaging kernels are weighted towards the free troposphere, where the relative

importance of hemispheric versus local trends is greater. However, our simulations indicate that this effect is insufficient to explain the negative trends over China. While this likely indicates a too positive emission trend for China, several other factors play a role in the model-observation mismatch. We find that the time-dependent MOPITT averaging kernels, combined with the low bias in simulated CO, provides a positive component to the simulated trends. Large anomalies in the simulated ozone column in the GMI CTM simulations also contribute a positive component to the northern hemisphere trends due to their impact on OH.

Variability in emissions is the primary driver of year-to-year variability in simulated CO, but OH variability also plays a role. The simulated OH is anti-correlated with both CO and the total ozone column, highlighting the importance of realistic overhead ozone columns for accurately simulating CO variability and trends. In addition, further work is needed to understand recent changes in CO emissions from China.

Acknowledgements

This work was supported by NASA's Modeling, Analysis, and Prediction program and computing resources from the NASA High-End Computing Program. We thank Bruce Van Aartsen for contributing to the GMI simulations. The CESM project is supported by the National Science Foundation and the Office of Science (BER) of the US Department of Energy. The MOPITT project is supported by the NASA Earth Observing System (EOS) Program. The National Center for Atmospheric Research (NCAR) is sponsored by the National Science Foundation.

Angelbratt, J., Mellqvist, J., Simpson, D., Jonson, J., Blumenstock, T., Borsdorff, T., Duchatelet, P., Forster, F., Hase, F., Mahieu, E., De Maziere, M., Notholt, J., Petersen, A., Raffalski, U., Servais, C., Sussmann, R., Warneke, T., and Vigouroux, C.: Carbon monoxide (CO) and ethane (C2H6) trends from ground-based solar FTIR measurements at six European stations, comparison and sensitivity analysis with the EMEP model, Atmospheric Chemistry and Physics, 11, 9253-9269, 10.5194/acp-11-9253-2011, 2011.

Bey, I., Jacob, D., Logan, J., and Yantosca, R.: Asian chemical outflow to the Pacific in spring: Origins, pathways, and budgets, Journal of Geophysical Research-Atmospheres, 106, 23097-23113, 10.1029/2001JD000806, 2001.

Crutzen, P.: A Discussion of the Chemistry of Some Minor Constituents in the Stratosphere and Troposphere, Pure and Applied Geophysics, 106, 1385-1399, 10.1007/BF00881092, 1973.
Deeter, M., Emmons, L., Edwards, D., Gille, J., and Drummond, J.: Vertical resolution and information content of CO profiles retrieved by MOPITT, Geophysical Research Letters, 31, 10.1029/2004GL020235, 2004.
Deeter, M. N.: MOPITT (Measurements of Pollution in the Troposphere) Validated Version 4 Product User's Guide, National Center for Atmospheric Research. Available at http://web3.acd.ucar.edu/mopitt/v4_users_guide_val.pdf, 2009.
Deeter, M. N., Martinez-Alonso, S., Edwards, D. P., Emmons, L. K., Gille, J. C., Worden, H. M., Pittman, J. V., Daube, B. C., and Wofsy, S. C.: Validation of MOPITT Version 5 thermal-infrared, near-infrared, and multispectral carbon monoxide profile retrievals for 2000-2011, Journal of Geophysical Research-Atmospheres, 118, 6710-6725, 10.1002/jgrd.50272, 2013.
Duncan, B. N., Strahan, S. E., Yoshida, Y., Steenrod, S. D., and Livesey, N.: Model study of the cross-tropopause transport of biomass burning pollution, Atmospheric Chemistry and Physics, 7, 3713-3736, 2007.
Duncan, B. N., and Logan, J. A.: Model analysis of the factors regulating the trends and variability of carbon monoxide between 1988 and 1997, Atmospheric Chemistry and Physics, 8, 7389-7403, 2008.
Edwards, D. P., Emmons, L. K., Hauglustaine, D. A., Chu, D. A., Gille, J. C., Kaufman, Y. J., Petron, G., Yurganov, L. N., Giglio, L., Deeter, M. N., Yudin, V., Ziskin, D. C., Warner, J., Lamarque, J. F., Francis, G. L., Ho, S. P., Mao, D., Chen, J., Grechko, E. I., and Drummond, J. R.: Observations of carbon monoxide and aerosols from the Terra satellite: Northern Hemisphere variability, Journal of Geophysical Research-Atmospheres, 109, 10.1029/2004jd004727, 2004.
EPA: Our Nation's Air - Status and Trends through 2010, edited by: EPA-454/R-12-001, Research Triangle Park, NC, 2011.
Eyring, V., Lamarque, J.-F., Hess, P., Arfeuille, F., Bowman, K., Chipperfiel, M. P., Duncan, B., Fiore, A., Gettelman, A., and Giorgetta, M. A.: Overview of IGAC/SPARC Chemistry-Climate Model Initiative (CCMI) community simulations in support of upcoming ozone and climate assessments, Sparc Newsletter, 40, 48-66, 2013.
Frith, S., Kramarova, N., Stolarski, R., McPeters, R., Bhartia, P., and Labow, G.: Recent changes in total column ozone based on the SBUV Version 8.6 Merged Ozone Data Set, Journal of Geophysical Research: Atmospheres, 119, 9735-9751, 2014.
Granier, C., Bessagnet, B., Bond, T., D'Angiola, A., van der Gon, H. D., Frost, G. J., Heil, A., Kaiser, J. W., Kinne, S., Klimont, Z., Kloster, S., Lamarque, J. F., Liousse, C., Masui, T., Meleux, F., Mieville, A., Ohara, T., Raut, J. C., Riahi, K., Schultz, M. G., Smith, S. J., Thompson, A., van Aardenne, J., van der Werf, G. R., and van Vuuren, D. P.: Evolution of anthropogenic and biomass burning emissions of air pollutants at global and regional scales during the 1980-2010 period, Climatic Change, 109, 163-190, 10.1007/s10584-011-0154-1, 2011.
Gratz, L., Jaffe, D., and Hee, J.: Causes of increasing ozone and decreasing carbon monoxide in springtime at the Mt. Bachelor Observatory from 2004 to 2013, Atmospheric Environment, 109, 323-330, 10.1016/j.atmosenv.2014.05.076, 2015.

Deleted: RUTZEN
Deleted: ISCUSSION
Deleted: OF
Deleted: HEMISTRY
Deleted: OF
Deleted: OME
Deleted: INOR
Deleted: ONSTITUENTS
Deleted: IN
Deleted: TRATOSPHERE
Deleted: AND
Deleted: ROPOSPHERE

Guenther, A., Jiang, X., Heald, C., Sakulyanontvittaya, T., Duhl, T., Emmons, L., and Wang, X.: The Model of Emissions of Gases and Aerosols from Nature version 2.1 (MEGAN2. 1): an extended and updated framework for modeling biogenic emissions, 2012.

He, H., Stehr, J., Hains, J., Krask, D., Doddridge, B., Vinnikov, K., Canty, T., Hosley, K., Salawitch, R., and Worden, H.: Trends in emissions and concentrations of air pollutants in the lower troposphere in the Baltimore/Washington airshed from 1997 to 2011, Atmospheric Chemistry and Physics, 13, 7859-7874, 2013.

Kurokawa, J., Ohara, T., Morikawa, T., Hanayama, S., Janssens-Maenhout, G., Fukui, T., Kawashima, K., and Akimoto, H.: Emissions of air pollutants and greenhouse gases over Asian regions during 2000-2008: Regional Emission inventory in ASia (REAS) version 2, Atmospheric Chemistry and Physics, 13, 11019-11058, 10.5194/acp-13-11019-2013, 2013.

Lamarque, J.F., Bond, T.C., Eyring, V., Granier, C., Heil, A., Klimont, Z., Lee, D., Liousse, C., Mieville, A., Owen, B. and Schultz, M.G.: Historical (1850–2000) gridded anthropogenic and biomass burning emissions of reactive gases and aerosols: methodology and application, Atmospheric Chemistry and Physics, 10, 7017-7039, 2010.

Li, L., and Liu, Y.: Space-borne and ground observations of the characteristics of CO pollution in Beijing, 2000–2010, Atmospheric Environment, 45, 2367-2372, http://dx.doi.org/10.1016/j.atmosenv.2011.02.026, 2011.

Naik, V., Voulgarakis, A., Fiore, A. M., Horowitz, L. W., Lamarque, J. F., Lin, M., Prather, M. J., Young, P. J., Bergmann, D., Cameron-Smith, P. J., Cionni, I., Collins, W. J., Dalsoren, S. B., Doherty, R., Eyring, V., Faluvegi, G., Folberth, G. A., Josse, B., Lee, Y. H., MacKenzie, I. A., Nagashima, T., van Noije, T. P. C., Plummer, D. A., Righi, M., Rumbold, S. T., Skeie, R., Shindell, D. T., Stevenson, D. S., Strode, S., Sudo, K., Szopa, S., and Zeng, G.: Preindustrial to present-day changes in tropospheric hydroxyl radical and methane lifetime from the Atmospheric Chemistry and Climate Model Intercomparison Project (ACCMIP), Atmospheric Chemistry and Physics, 13, 5277-5298, 10.5194/acp-13-5277-2013, 2013.

Ohara, T., Akimoto, H., Kurokawa, J., Horii, N., Yamaji, K., Yan, X., and Hayasaka, T.: An Asian emission inventory of anthropogenic emission sources for the period 1980-2020, Atmospheric Chemistry and Physics, 7, 4419-4444, 2007.

Oman, L. D., Ziemke, J. R., Douglass, A. R., Waugh, D. W., Lang, C., Rodriguez, J. M., and Nielsen, J. E.: The response of tropical tropospheric ozone to ENSO, Geophysical Research Letters, 38, 10.1029/2011gl047865, 2011.

Reynolds, R., Rayner, N., Smith, T., Stokes, D., and Wang, W.: An improved in situ and satellite SST analysis for climate, Journal of Climate, 15, 1609-1625, 10.1175/1520-0442(2002)015<1609:AIISAS>2.0.CO;2, 2002.

Riahi, K., Grübler, A., and Nakicenovic, N.: Scenarios of long-term socio-economic and environmental development under climate stabilization, Technological Forecasting and Social Change, 74, 887-935, 2007.

Rienecker, M. M., Suarez, M. J., Gelaro, R., Todling, R., Bacmeister, J., Liu, E., Bosilovich, M. G., Schubert, S. D., Takacs, L., Kim, G.-K., Bloom, S., Chen, J., Collins, D., Conaty, A., da Silva, A., Gu, W., Joiner, J., Koster, R. D., Lucchesi, R., Molod, A., Owens, T., Pawson, S., Pegion, P., Redder, C. R., Reichle, R., Robertson, F. R., Ruddick, A. G., Sienkiewicz, M., and Woollen, J.: MERRA: NASA's Modern-Era Retrospective

Formatted: Font:Not Italic

Formatted: Font:Not Italic

Analysis for Research and Applications, Journal of Climate, 24, 3624-3648, 10.1175/JCLI-D-11-00015.1, 2011.
Stein, O., Schultz, M., Bouarar, I., Clark, H., Huijnen, V., Gaudel, A., George, M., and Clerbaux, C.: On the wintertime low bias of Northern Hemisphere carbon monoxide found in global model simulations, Atmospheric Chemistry and Physics, 14, 9295-9316, 10.5194/acp-14-9295-2014, 2014.
Steinbrecht, W., Köhler, U., Claude, H., Weber, M., Burrows, J.P., and van der A, R.J.: Very high ozone columns at northern mid-latitudes in 2010, Geophysical Research Letters, 38, 10.1029/2010GL046634, 2011.
Strahan, S. E., Duncan, B. N., and Hoor, P.: Observationally derived transport diagnostics for the lowermost stratosphere and their application to the GMI chemistry and transport model, Atmospheric Chemistry and Physics, 7, 2435-2445, 2007.
Strode, S., Duncan, B., Yegorova, E., Kouatchou, J., Ziemke, J., and Douglass, A.: Implications of carbon monoxide bias for methane lifetime and atmospheric composition in chemistry climate models, Atmospheric Chemistry and Physics, 15, 11789-11805, 2015a.
Strode, S. A., Rodriguez, J. M., Logan, J. A., Cooper, O. R., Witte, J. C., Lamsal, L. N., Damon, M., Van Aartsen, B., Steenrod, S. D., and Strahan, S. E.: Trends and variability in surface ozone over the United States, Journal of Geophysical Research: Atmospheres, 120, 9020-9042, 2015b.
Thompson, A.: The Oxidizing Capacity of the Earth's Atmosphere: Prsobable Past and Future Change, Science, 256, 1157-1165, 10.1126/science.256.5060.1157, 1992.
Tilmes, S., Lamarque, J. F., Emmons, L. K., Kinnison, D. E., Marsh, D., Garcia, R. R., Smith, A. K., Neely, R. R., Conley, A., Vitt, F., Val Martin, M., Tanimoto, H., Simpson, I., Blake, D. R., and Blake, N.: Representation of the Community Earth System Model (CESM1) CAM4-chem within the Chemistry-ClimateModel Initiative (CCMI), Geosci. Model Dev. Discuss., 2016, 1-50, 10.5194/gmd-2015-237, 2016.
Tohjima, Y., Kubo, M., Minejima, C., Mukai, H., Tanimoto, H., Ganshin, A., Maksyutov, S., Katsumata, K., Machida, T., and Kita, K.: Temporal changes in the emissions of CH4 and CO from China estimated from CH4/CO2 and CO/CO2 correlations observed at Hateruma Island, Atmospheric Chemistry and Physics, 14, 1663-1677, 10.5194/acp-14-1663-2014, 2014.
van der Werf, G. R., Randerson, J. T., Giglio, L., Collatz, G. J., Kasibhatla, P.S., and Arellano, Jr., A.F.: Interannual variability in global biomass burning emissions from 1997-2004, Atmospheric Chemistry and Physics, 6, 3423-3441, 2006.
van der Werf, G. R., Randerson, J. T., Giglio, L., Collatz, G. J., Mu, M., Kasibhatla, P. S., Morton, D. C., DeFries, R. S., Jin, Y., and van Leeuwen, T. T.: Global fire emissions and the contribution of deforestation, savanna, forest, agricultural, and peat fires (1997-2009), Atmospheric Chemistry and Physics, 10, 11707-11735, 10.5194/acp-10-11707-2010, 2010.
van Donkelaar, A., Martin, R. V., Leaitch, W. R., Macdonald, A. M., Walker, T. W., Streets, D. G., Zhang, Q., Dunlea, E. J., Jimenez, J. L., Dibb, J. E., Huey, L. G., Weber, R., and Andreae, M. O.: Analysis of aircraft and satellite measurements from the Intercontinental Chemical Transport Experiment (INTEX-B) to quantify long-range transport of East Asian sulfur to Canada, Atmospheric Chemistry and Physics, 8, 2999-3014, 2008.

Formatted: Font:(Default) Times New Roman, Not Bold

Deleted: HOMPSON
Deleted: HE
Deleted: XIDIZING
Deleted: APACITY
Deleted: OF
Deleted: THE
Deleted: ARTHS
Deleted: TMOSPHERE
Deleted: -
Deleted: ROBABLE
Deleted: AST
Deleted: AND
Deleted: UTURE
Deleted: HANGES

576 Voulgarakis, A., Marlier, M., Faluvegi, G., Shindell, D., Tsigaridis, K., and Mangeon, S.:
577 Interannual variability of tropospheric trace gases and aerosols: The role of biomass
578 burning emissions, Journal of Geophysical Research-Atmospheres, 120, 7157-7173,
579 10.1002/2014JD022926, 2015.
580 Wang, Y., Munger, J., Xu, S., McElroy, M., Hao, J., Nielsen, C., and Ma, H.: CO2 and its
581 correlation with CO at a rural site near Beijing: implications for combustion efficiency in
582 China, Atmospheric Chemistry and Physics, 10, 8881-8897, 10.5194/acp-10-8881-2010,
583 2010.
584 Warner, J., Carminati, F., Wei, Z., Lahoz, W., and Attie, J.: Tropospheric carbon
585 monoxide variability from AIRS under clear and cloudy conditions, Atmospheric
586 Chemistry and Physics, 13, 12469-12479, 10.5194/acp-13-12469-2013, 2013.
587 Worden, H. M., Cheng, Y., Pfister, G., Carmichael, G. R., Zhang, Q., Streets, D. G.,
588 Deeter, M., Edwards, D. P., Gille, J. C., and Worden, J. R.: Satellite-based estimates of
589 reduced CO and CO2 emissions due to traffic restrictions during the 2008 Beijing
590 Olympics, Geophysical Research Letters, 39, 2012.
591 Worden, H. M., Deeter, M. N., Frankenberg, C., George, M., Nichitiu, F., Worden, J.,
592 Aben, I., Bowman, K. W., Clerbaux, C., Coheur, P. F., de Laat, A. T. J., Detweiler, R.,
593 Drummond, J. R., Edwards, D. P., Gille, J. C., Hurtmans, D., Luo, M., Martinez-Alonso,
594 S., Massie, S., Pfister, G., and Warner, J. X.: Decadal record of satellite carbon monoxide
595 observations, Atmospheric Chemistry and Physics, 13, 837-850, 10.5194/acp-13-837-
596 2013, 2013.
597 Yin, Y., Chevallier, F., Ciais, P., Broquet, G., Fortems-Cheiney, A., Pison, I., and
598 Saunois, M.: Decadal trends in global CO emissions as seen by MOPITT, Atmos. Chem.
599 Phys., 15, 13433-13451, 10.5194/acp-15-13433-2015, 2015.
600 Yoon, J., Pozzer, A., Hoor, P., Chang, D., Beirle, S., Wagner, T., Schloegl, S., Lelieveld,
601 J., and Worden, H.: Technical Note: Temporal change in averaging kernels as a source of
602 uncertainty in trend estimates of carbon monoxide retrieved from MOPITT, Atmospheric
603 Chemistry and Physics, 13, 11307-11316, 10.5194/acp-13-11307-2013, 2013.
604 Yoon, J., and Pozzer, A.: Model-simulated trend of surface carbon monoxide for the
605 2001-2010 decade, Atmospheric Chemistry and Physics, 14, 10465-10482, 10.5194/acp-
606 14-10465-2014, 2014.
607 Yumimoto, K., Uno, I., and Itahashi, S.: Long-term inverse modeling of Chinese CO
608 emission from satellite observations, Environmental Pollution, 195, 308-318,
609 10.1016/j.envpol.2014.07.026, 2014.
610 Zhang, Q., Streets, D. G., Carmichael, G. R., He, K. B., Huo, H., Kannari, A., Klimont,
611 Z., Park, I. S., Reddy, S., Fu, J. S., Chen, D., Duan, L., Lei, Y., Wang, L. T., and Yao, Z.
612 L.: Asian emissions in 2006 for the NASA INTEX-B mission, Atmospheric Chemistry
613 and Physics, 9, 5131-5153, 2009.
614 Zhao, Y., Nielsen, C. P., McElroy, M. B., Zhang, L., and Zhang, J.: CO emissions in
615 China: Uncertainties and implications of improved energy efficiency and emission
616 control, Atmospheric Environment, 49, 103-113, 10.1016/j.atmosenv.2011.12.015, 2012.
617

618

Table 1: Description of Simulations

Simulation	Model	Meteorology	Anthropogenic Emissions	Biomass Burning Emissions
G-Ref-C1	GEOSCCM	internally derived	MACCity	MACCity, GFED3 (2009-2010)
C-Ref-C1	CAM4-Chem	internally derived	MACCity	MACCity, then repeat 2008
Ref-C1-SD	GMI	MERRA	MACCity	Same as GEOSCCM
EmFix	GMI	MERRA	Fixed at 2000	Fixed at 2000
AltEmis	GMI	MERRA	Strode et al [2015]	GFED3

Deleted: CITY
Deleted: ITY
Deleted: ITY
Deleted: ITY
Deleted: ITY

Table 2: Regional Trends and Correlations

a. Trends[1,2]

	Years	E. USA	Europe	E. China	N. Hemisphere
G-Ref-C1[3]	2000-2010	-2.2 (0.38)	-1.8 (0.42)	2.2 (1.1)	-0.76 (3.0)
C-Ref-C1[3]	2000-2010	-3.4 (0.54)	-2.9 (0.50)	1.4 (1.4)	-0.90 (3.0)
Ref-C1-SD[3]	2000-2010	-2.4 (0.53)	-1.6 (0.59)	1.4 (1.1)	-0.76 (3.0)
EmFix[3]	2000-2010	1.3 (0.55)	1.5 (0.44)	2.1 (0.87)	0.96 (2.5)
AltEmis[3]	2000-2010	0.71 (0.73)	0.74 (0.66)	3.8 (1.4)	1.1 (3.4)
MOPITT	*2000-2010*	*-2.5 (0.64)*	*-1.8 (0.69)*	*-2.9 (1.8)*	*-1.4 (2.8)*
MOPITT	*2000-2014*	*-2.1 (0.41)*	*-1.7 (0.43)*	*-3.1 (1.1)*	*-1.4 (1.7)*

[1] 10^{16} molec cm^{-2} yr^{-1}

[2] 1-sigma uncertainty given in parentheses

[3] Simulation results convolved with MOPITT averaging kernel and a priori

b. Correlation coefficient (r) with monthly MOPITT anomalies[1,2]

	Years	E. USA	Europe	E. China	N. Hemisphere
G-Ref-C1	2000-2010	**0.26**	**0.39**	0.061	**0.71**
C-Ref-C1	2000-2010	0.23	**0.36**	0.18	**0.62**
Ref-C1-SD	2000-2010	**0.43**	**0.51**	**0.39**	**0.73**
EmFix	2000-2010	0.10	0.21	0.071	0.059
AltEmis	2000-2010	**0.55**	**0.59**	**0.48**	**0.69**

[1] Correlations are calculated from the de-trended and de-seasonalized time series.

[2] Statistically significant correlations at the 95% confidence level are indicated in bold.

Deleted: G-Ref-C1[3] ... [1]

Formatted: Font:Bold

Formatted: Font:Bold

Formatted: Font:Bold

Formatted: Font:Bold

Formatted: Font:Bold

Formatted: Font:Bold

Deleted: G-Ref-C1 ... [2]

Formatted: Superscript

Page 18: [1] DeletedStrode, Sarah A. (GSFC-614.0)[UNIVERSITIES SPACE RESEARCH ASSOCIATION] 4/20/16 10:56 AM

G-Ref-C1[3]	2000-2011	-2.4 (0.33)	-1.9 (0.36)	1.9 (0.97)	-0.90 (2.5)
Ref-C1-SD[3]	2000-2011	-2.1 (0.43)	-1.7 (0.51)	1.3 (1.0)	-0.89 (2.6)
EmFix[3]	2000-2011	1.3 (0.43)	1.3 (0.39)	2.0 (0.79)	0.91 (2.1)
AltEmis[3]	2000-2011	0.56 (0.59)	0.50 (0.58)	3.3 (1.3)	0.89 (2.9)
MOPITT	*2000-2011*	*-2.5 (0.55)*	*-1.9 (0.59)*	*-2.9 (1.5)*	*-1.5 (2.4)*

Page 18: [2] DeletedStrode, Sarah A. (GSFC-614.0)[UNIVERSITIES SPACE RESEARCH ASSOCIATION] 4/20/16 10:56 AM

G-Ref-C1	2000-2011	0.25	0.37	0.046	0.72
Ref-C1-SD	2000-2011	0.41	0.51	0.36	0.73
EmFix	2000-2011	0.095	0.24	0.080	0.094
AltEmis	2000-2011	0.53	0.59	0.47	0.69

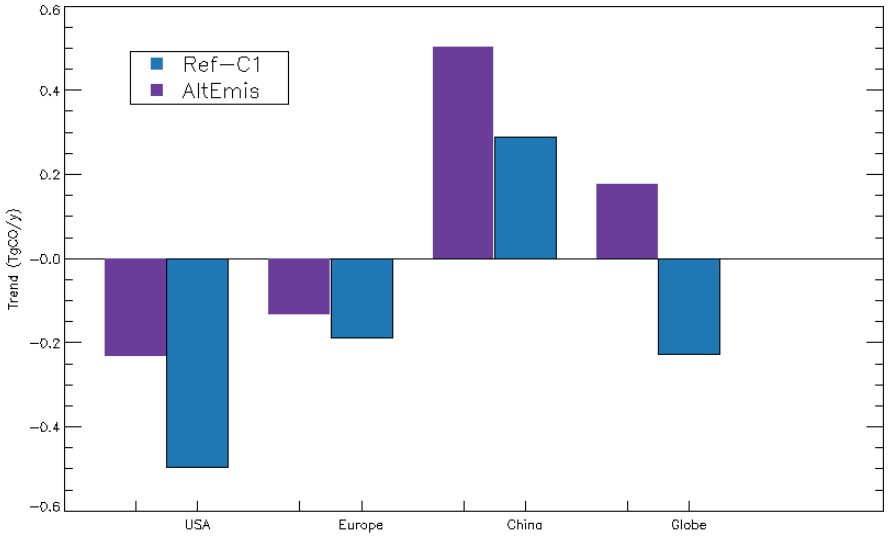

Figure 1: Trends in the CO emissions used in the Ref-C1 and Ref-C1-SD simulations (blue bars) and AltEmis simulation (purple bars) over 2000-2010 for the United States, Europe, China, and the world.

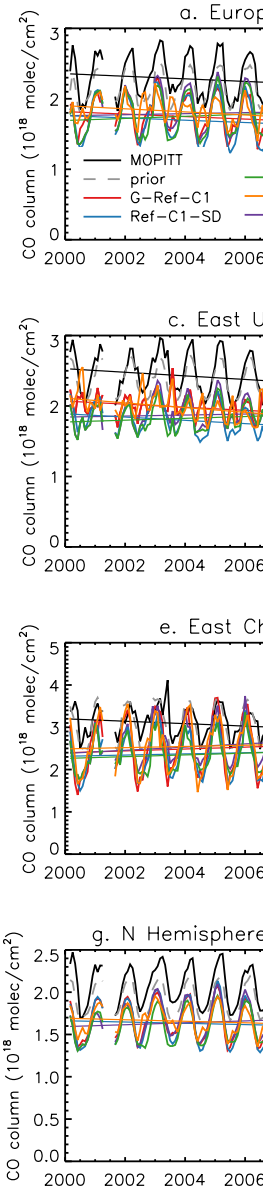

Deleted:

Formatted: Font:(Default) Times New Roman

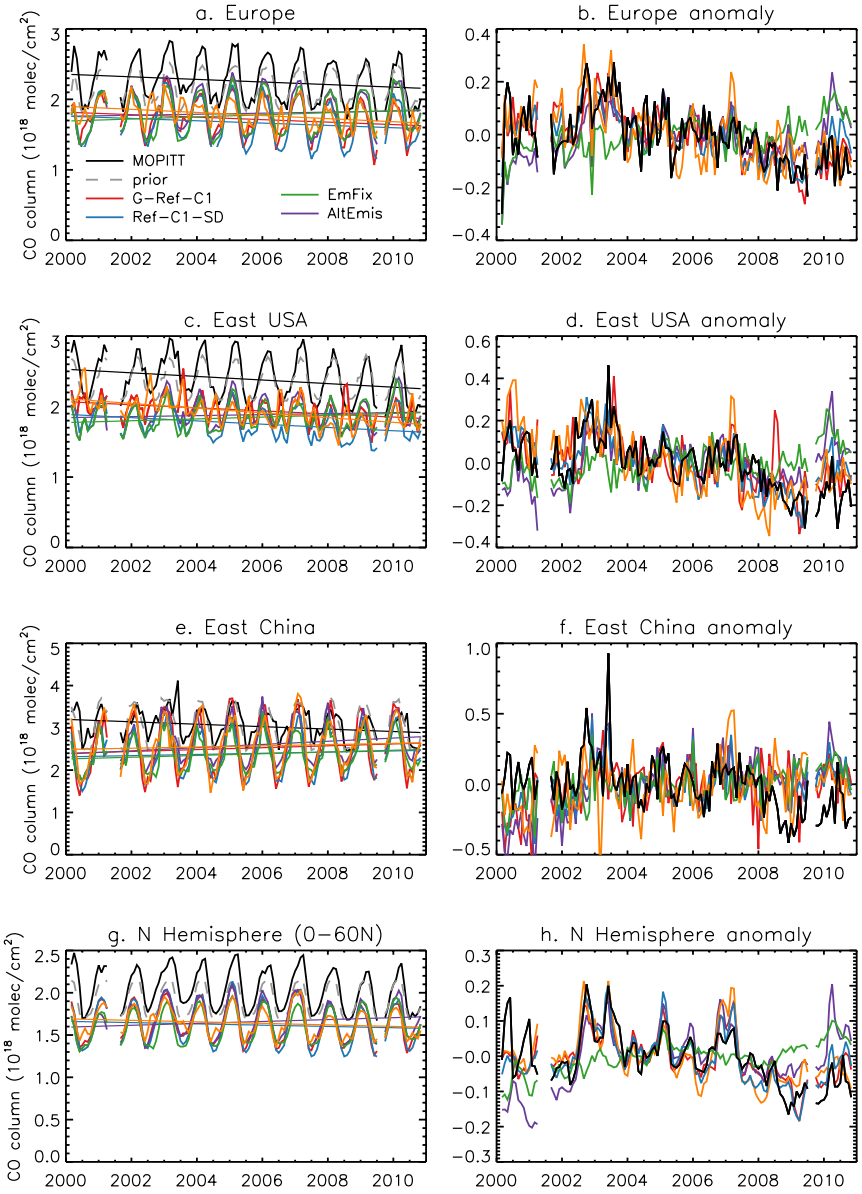

Figure 2: The time series and trends (left column) and de-seasonalized monthly anomalies (right column) of the CO column from MOPITT (black), the MOPITT a priori (gray), and simulated by G-Ref-C1 (red), Ref-C1-SD (blue), EmFix (green), C-Ref-C1 (orange), and AltEmis (purple) for 2000-2010. The regions shown are (a,b) Europe (0°-

Formatted: Font:(Default) Times New Roman, Bold

Formatted: Font:(Default) Times New Roman

15°E, 45°-55°N), (c,d) eastern U.S.A. (95°-75°W, 35°-40°N), (e,f) eastern China (110°-123°E, 30°-40°N), and (g,h) the northern hemisphere (0°-60°N).

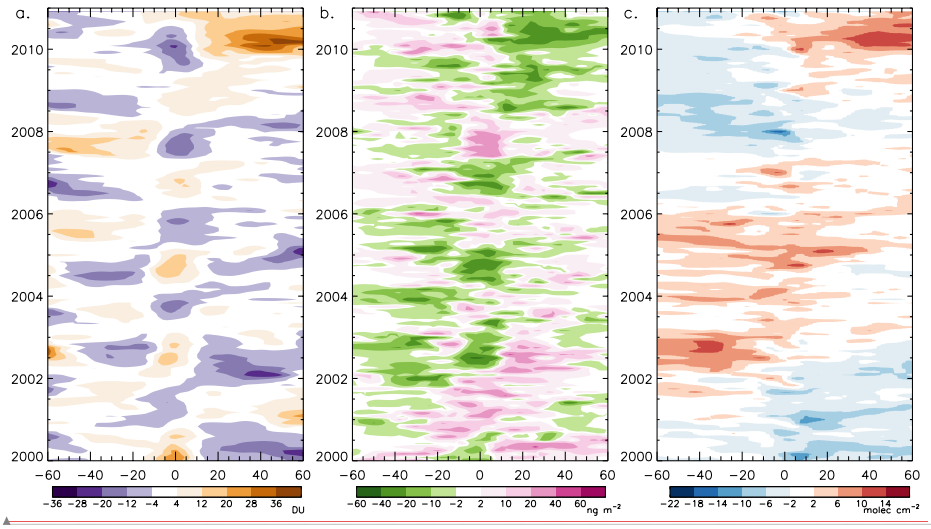

Figure 3: Deseasonalized monthly anomalies in the total ozone column (left), mean tropospheric OH (center), and CO column (right) from the EmFix simulation as a function of latitude and month.

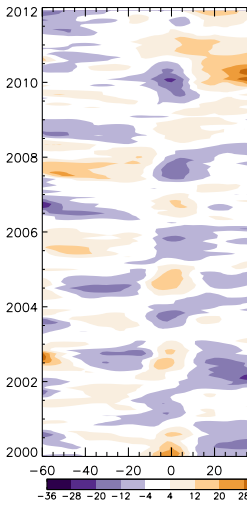

Deleted:

Formatted: Font:(Default) Times New Roman

Formatted: Font:(Default) Times New Roman

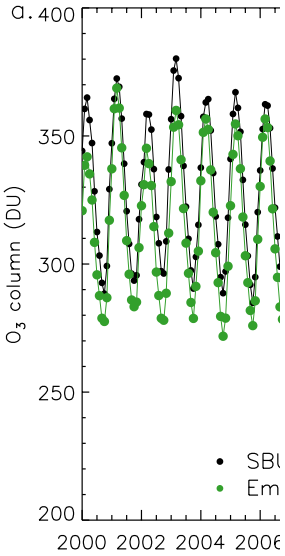

Deleted:

Formatted: Font:(Default) Times New Roman

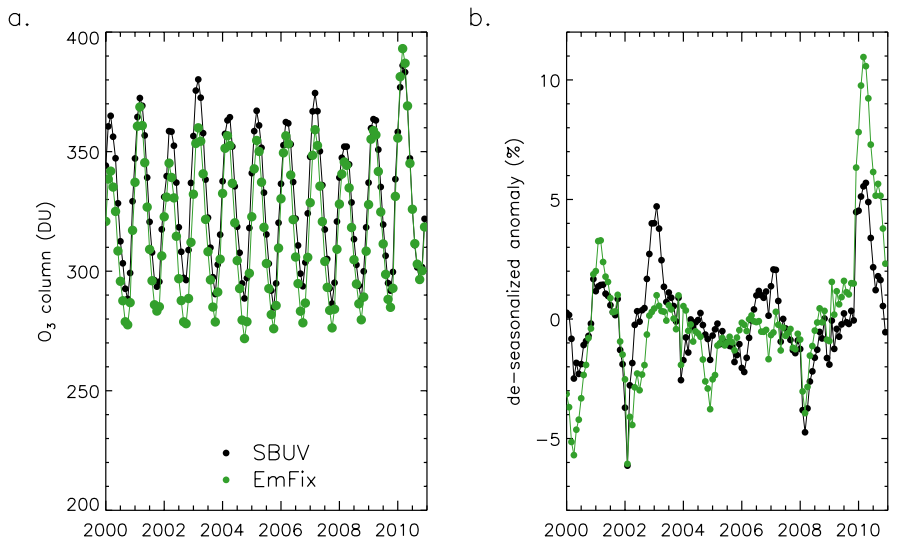

Figure 4: Monthly ozone column (a) and de-seasonalized ozone column anomaly (b) in SBUV data (black) and the EmFix simulation (green) for 30°-60°N.

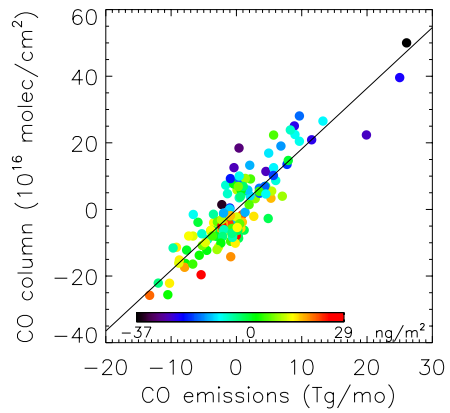

Figure 5: Monthly simulated CO column anomalies from the Ref-C1-SD simulation as a function of CO emissions for 10°S-10°N. Colors indicate the simulated OH column anomaly for the given month.

Formatted: Font:(Default) Times New Roman

Deleted:

Formatted: Font:(Default) Times New Roman

Formatted: Font:(Default) Times New Roman

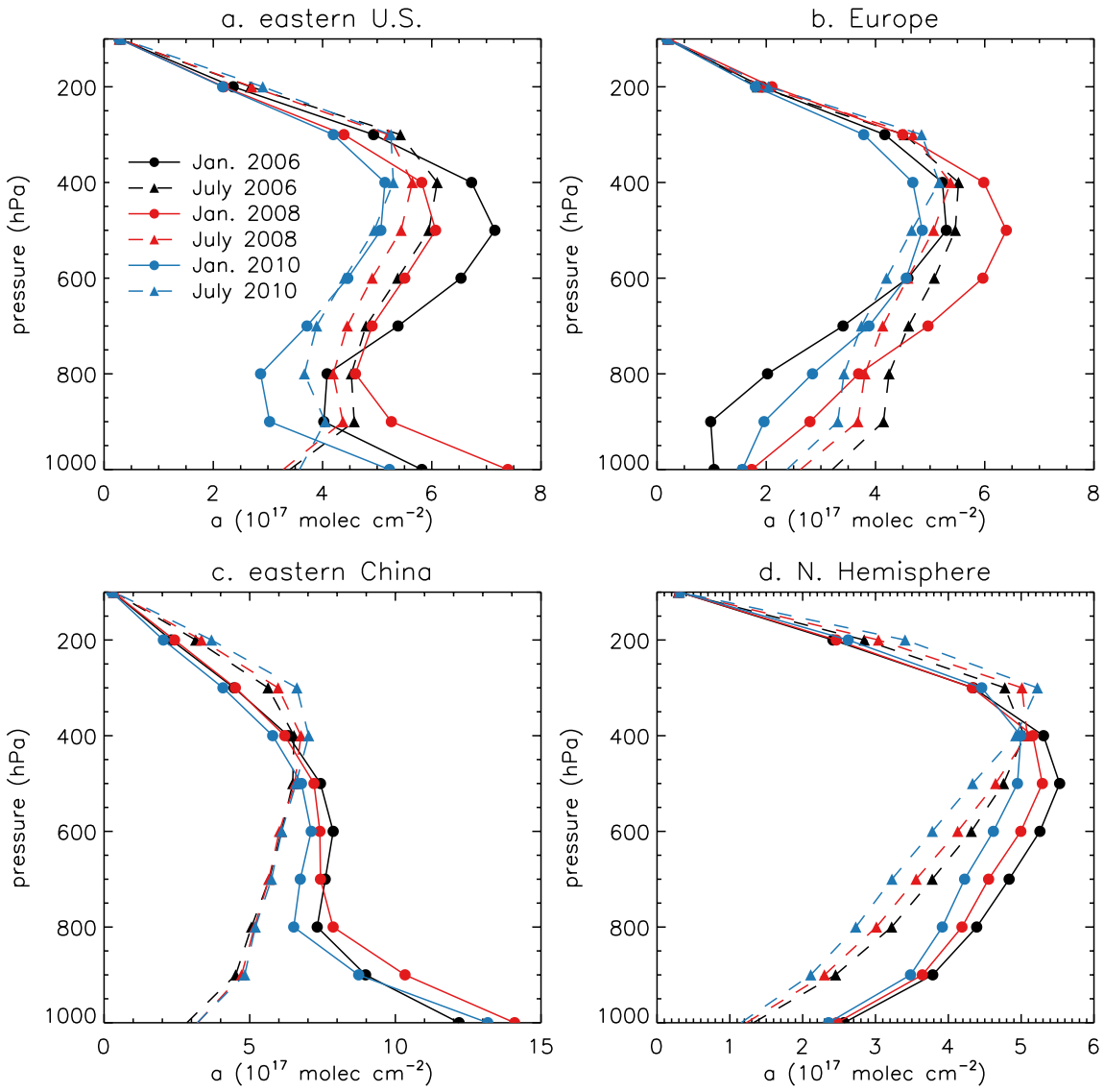

Supplemental Figure S1: Regionally averaged monthly column averaging kernels for January (circles) and July (triangles) for 2006 (black), 2008 (red), and 2010 (blue) for (a) the eastern United States, (b) Europe, (c) eastern China, and (d) the northern hemisphere. The region definitions are the same as in Fig. 2.